International Journal of Medical Microbiology 309 (2019) 151323

Contents lists available at ScienceDirect

International Journal of Medical Microbiology

journal homepage: www.elsevier.com/locate/ijmm

Assessing capreomycin resistance on *tlyA* deficient and point mutation (G695A) *Mycobacterium tuberculosis* strains using multi-omics analysis

Jiao Zhao[b,1], Wenjing Wei[a,1], Huimin Yan[c], Ying Zhou[d], Zhenyan Li[e], Yanmei Chen[a], Chenchen Zhang[a], Jincheng Zeng[c,*], Tao Chen[a,f,*], Lin Zhou[a,b,*]

[a] Center for Tuberculosis Control of Guangdong Province, Key Laboratory of Translational Medicine of Guangdong, Guangzhou 510630, China
[b] Jinan University, Guangzhou 510632, China
[c] Dongguang Key Laboratory of Medical Bioactive Molecular Development and Translational Research, Guangdong Provincial Key Laboratory of Medical Molecular Diagnostics, Guangdong Medical University, Dongguan, Guangdong, 523808, China
[d] School of Stomatology and Medicine, Foshan University, Foshan, Guangdong, 528000, China
[e] The First Affiliated Hospital, Jinan University, Guangzhou 510630, China
[f] South China Institute of Biomedicine, Guangzhou 510530, China

ARTICLE INFO

Keywords:
Mycobacterium tuberculosis
tlyA
Capreomycin
Multi-omics
S-adenosyl-L-methionine-dependent methyltransferase

ABSTRACT

Capreomycin (CAP), a cyclic peptide antibiotic, is considered to be an ideal second-line drug for tuberculosis (TB). However, in the past few years, the emergence of more CAP-resistant (CAP^r) TB patients has limited its use. Although it has been reported that CAP resistance to *Mycobacterium tuberculosis* (Mtb) is associated with *rrs* or *tlyA* mutation, the exact mechanism of CAP^r Mtb strains, especially the mechanism associated with *tlyA* deficient or mutation, is not fully understood. Herein, we utilized a multi-omics (genome, proteome, and metabolome) approach to assess CAP resistance on *tlyA* deficient CAP^r Mtb strains (CAP^r1) and *tlyA* point mutation CAP^r Mtb strains (CAP^r2) that we established for the first time *in vitro* to investigate the CAP-resistant mechanism. Our results showed that the CAP^r1 strains (> 40 μg/ml) was more resistant to CAP than the CAP^r2 strains (G695A, 10 μg/ml). Furthermore, multi-omics analysis indicated that the CAP^r1 strains exhibited greater drug tolerance than the CAP^r2 strains may be associated with the weakening of S-adenosyl-L-methionine-dependent methyltransferase (AdoMet-MT) activity and abnormal membrane lipid metabolism such as suppression of fatty acid metabolism, promotion of glycolipid phospholipid and glycerolipid metabolism. As a result, these studies reveal a new mechanism for CAP resistance to *tlyA* deficient or mutation Mtb strains, and may be helpful in developing new therapeutic approaches to prevent Mtb resistance to CAP.

1. Introduction

Tuberculosis (TB) caused by Mycobacterium tuberculosis (Mtb) is a deadly bacterial disease that infects approximately one-third of the world's population through its symptomatic or asymptomatic status. In particular, the emergence of multidrug-resistant TB (MDR-TB) and extensively drug-resistant TB (XDR-TB) patients exacerbates the severity of this public health and safety crisis (WHO, 2017). Although second-line anti-TB injectable drugs such as aminoglycosides kanamycin, amikacin, capreomycin and viomycin have been widely used to improve treatment outcomes of MDR-TB (Caminero et al., 2010), there are still more MDR-TB patients who are resistant to the above drugs (Falzon et al., 2011).

Capreomycin (CAP) is considered as a second-line drug for TB and is also a representative of peptide anti-TB drugs. It is known that the resistance of Mtb to CAP is related to *rrs* or *tlyA* mutation (Akbergenov et al., 2011; Maus et al., 2005; Monshupanee et al., 2012). Anna Engström et al. reported that Mtb with *rrs* mutation might be more sensitive to CAP than Mtb with *tlyA* mutation based on clinical sequencing data (Engstrom et al., 2011). Notably, some TB patients show cross-resistance to CAP, amikacin and kanamycin, and *rrs* A1401 G allele of Mtb is a marker of cross-resistance to these drugs. Since amikacin and kanamycin are recommended as the first choice for second-line injectable anti-TB drugs, it is unclear whether any of these three drugs can induce *rrs* mutation.

Until recently, the detailed mechanism of *rrs* mutation in CAP-resistant (CAP^r) strains is unclear, except for founding the clinical CAP^r strains with *rrs* mutations. Certainly, the exact mechanism of CAP^r Mtb

* Corresponding authors.
E-mail addresses: zengjc@gdmu.edu.cn (J. Zeng), chentaoibp@163.com (T. Chen), zhoulingjk@163.com (L. Zhou).
[1] These authors contributed equally to this work.

https://doi.org/10.1016/j.ijmm.2019.06.003
Received 19 February 2019; Received in revised form 26 May 2019; Accepted 22 June 2019

strains which is associated with *tlyA* deficient or mutation, is not fully understood. *TlyA* encodes protein TlyA with rRNA methyltransferase activities, which catalyze 2'-O-methylation at nucleotides C1409 of 16*S* rRNA and C1920 of 23 s rRNA to offer the optimal CAP binding to the mycobacterial ribosome at the interface of the small and large subunits so as to inhibit mRNA-tRNA translocation (Stanley et al., 2010). It is known TlyA with loss-of-function mutations in rRNA methylation, can confer CAP resistance (Akbergenov et al., 2011; Maus et al., 2005; Monshupanee et al., 2012) and the complementation of a *tlyA*-deficient strain with a wild-type copy of *tlyA* restores CAP susceptibility to Mtb (Maus et al., 2005). Despite the critical role of TlyA in CAP sensitivity and the identification of inactivating mutations that cause resistance, our current understanding of TlyA structure and the mechanism of action as well as the relation between *rrs* mutations and *tlyA* mutations remains limited.

Recently, proteomics and metabolomics, representing the direct performer and final feedback of the overall function or state-of-the-life system, served as the basis for a better understanding of the drug resistant mechanisms and elucidating drug mechanisms and monitoring treatment outcomes (Luies et al., 2017a,b; Vranakis et al., 2014). In this study, a multi-omics approach, which integrates the genome, high-throughput isobaric tag for relative and absolute quantitation (iTRAQ)-based quantitative proteomics and liquid Chromatograph Mass Spectrometer (LC–MS)-based metabolomics, was performed to investigate the resistance mechanism of two different laboratory CAP-resistant Mtb strains, *tlyA* deficient CAP^r Mtb strains (CAP^r1) and *tlyA* point mutation CAP^r Mtb strains (CAP^r2).

This is the first study on the mechanism of CAP resistance in Mtb *in vitro* using the statistically integrated multi-omics method. In this study, we found that, except TlyA inactivation, *tlyA*-deficient Mtb has a more complex drug-resistant mechanism compared to a *tlyA* point-mutated Mtb, including the reduction of S-adenosyl-L-methionine-dependent methyltransferases (AdoMet-MTs) activity and abnormal membrane lipid metabolism such as inhibiting fatty acid metabolism but promoting glycolipid phospholipid and glycerolipid metabolism. The results of this study will advance our understanding of the mechanisms underlying the resistance of bacteria to antibiotics.

2. Materials and methods

2.1. Bacterial cultures

Mtb H37Rv strain was cultured on Löwenstein-Jensen (LJ) medium and were respectively treated with CAP, kanamycin (KAN) and amikacin (AMK) according to the route of Fig. 1 to obtain the corresponding drug-resistant Mtb. For Mtb treated with drugs, single colonies were randomly selected and cultured in liquid culture for the extraction of genomic DNA and testing minimum inhibitory concentrations (MIC) of Mtb strains according to the established protocols (Kim and Hong, 1992; Larsen et al., 2007; Wang et al., 2011). Then single colonies were assessed by targeted sequencing of PCR amplicons of *rrs* and *tlyA* genes. The primers used in the targeted sequencing are described in Supplemental Table S7 (see Supplemental Experimental Procedures).

2.2. Drug susceptibility testing

The MICs of the drugs were determined as described by Luciano Mengatto et al. (Mengatto et al., 2006). The detailed method was shown in Supplemental Experimental Procedures.

2.3. Congo red assay

When Mtb grew to stationary phase, 2 µl was dropped on 7H10 medium supplemented with 1.5% agar and 100 µg/ml Congo red (Sigma). The plates were incubated at 37 °C for colony morphology and

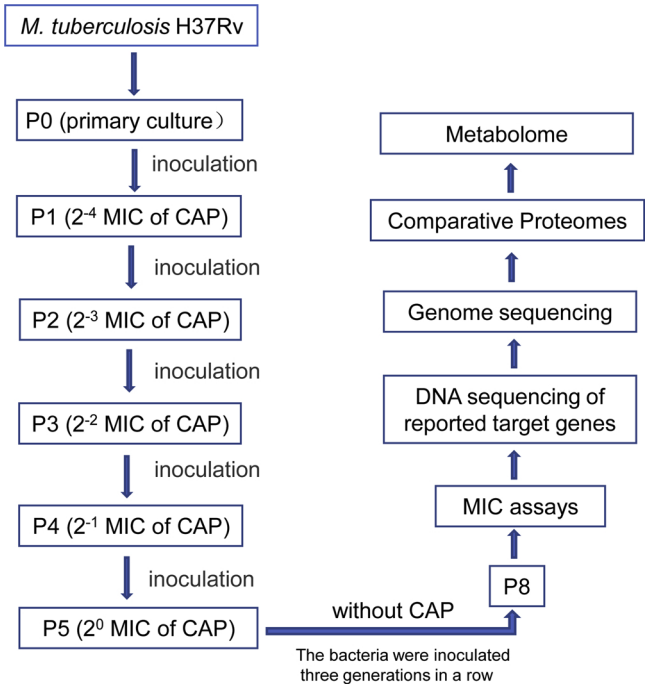

Fig. 1. The process of capreomycin-induced drug resistance. *M. tuberculosis* H37Rv strain was cultured on Löwenstein-Jensen (LJ) medium and processed by amplification culture named as passage 0 (P0) strains, which were selected for preparing CAP-resistant strains. Concentration gradients (2^{-4}, 2^{-3}, 2^{-2}, 2^{-1}, 2^{0}) of CAP based on the critical concentration (40.0 µg/mL CAP) contained LJ medium were prepared, and P0 strains (1 MCF) were cultured in LJ medium (2^{-4} CAP concentration) for approximately 4 weeks named as passage 1 (P1). Repeat this step till passage 4 (P5) strains, which met to the WHO criteria for CAP-resistant strains, and then the resistant strains were verified by the appropriate concentrations of drug used in the drug-susceptibility test. The resistant strains were continuously cultured to passage 8 (P8) without CAP, and then analyzed by the drug-susceptibility test. The single colonies were randomly selected and cultured in liquid culture for the extraction of genomic DNA and testing CAP MICs of Mtb strains. Then single colonies were assessed by targeted sequencing of PCR amplicons of genes associated with CAP resistance. The primers used in the targeted sequencing are described in Supplemental Table S7. Two strains, one *tlyA*-deficient and one *tlyA*-point mutant Mtb are identified and subjected to full genome resequencing, proteomic and metabolomic analysis.

Congo red staining (Deshayes et al., 2005; Sonden et al., 2005).

2.4. Sliding motility assay

Mtb strains were grown to stationary phase, 2 µl was dispensed on plate containing 7H9 medium with 0.3% agar. The plate was then incubated at 37 °C for 5 weeks (Deshayes et al., 2005; Sonden et al., 2005).

2.5. Whole genome resequencing

The Mtb genome was extracted as described by Somerville et al. PCR-free DNA libraries for full-genome sequencing were constructed from the genomic DNA of selected strains using a TruSeq DNA kit (Illumina, Inc.) according to the manufacturer's protocol, and assayed using the Illumina MiSeq or HiSeq 2000 sequencing systems. The detailed method was shown in Supplemental Experimental Procedures.

2.6. Protein preparation and iTRAQ labeling

The proteins were extracted using mechanical crushing method. For each sample, total protein (100 µg) was digested with 3.3 µl of trypsin

(1 μg/μl) at 37 °C for 24 h. After trypsin digestion, peptides were reconstituted in 0.5 M TEAB and processed according to the manufacturer's instructions (Applied Biosystems) (see Supplemental Experimental Procedures).

2.7. LC–MS analysis

The resolved peptides were submitted to MS on an Q EXACTIVE (Thermo Fisher Scientific, San Jose, CA, USA) with an analytical C18 column (75 μm i.d. × 150 mm, 2 μm, 100 Å, nano Viper, Thermo Fisher Scientific, USA) for identification and quantification. The raw data were searched with Proteome Discoverer v2.2 version (Thermo Scientific) against the H37Rv database with the same parameters setting as previously described. The final proteins that were seemed to be differentially expressed were filtered as a P value < 0.05 and 1.5-fold changes (> 1.50 or < 0.667) relative to the control group.

2.8. Macrophage virulence assay

Bacterial suspensions of CAP^{r}1, CAP^{r}2 and their parental strains were added respectively to wells containing RAW264.7 cells. The survival ability of bacteria inside macrophages was measured after cells were lysed at the times indicated (see Supplemental Experimental Procedures).

2.9. Metabolite extraction for LC–MS

The collected Mtb were quenched immediately by liquid nitrogen for 10 min stored at −80 °C. The intracellular metabolites in Mtb were extracted according to the method described by Loots du (Loots du, 2016) and the metabolites in the culture filtrate were extracted according to the method described by Lau, S. K. et al. (Lau et al., 2015) (See Supplemental Experimental Procedures).

2.10. Identification and analysis of metabolites by LC–MS

The samples were analyzed in the positive ion mode on an AB 5600 + Triple TOF mass spectrometer system coupled to an Ekspert UltraLC system (110, AB Sciex) which equipped with ACQUITY UPLC HSS T3 (1.8 μm 2.1 × 100 mm, Waters) column. The raw MS files (WIFF format file) were converted to ABF (analysis base file format) using the freely available Reifycs file converter (http://www.reifycs.com/AbfConverter/). Peak picking and alignment were performed using MS-DIAL version 2.24 and the parameters were set as follows: Alignment: MS1 tolerance, 0.01 Da; Retention time tolerance, 0.1 min; Identification: Accurate mass tolerance (MS1), 0.025 Da; Accurate mass tolerance (MS1), 0.25 Da. Representative MS/MS spectra were exported in abf format for MS-DIAL, and compound identification was performed against MS/MS libraries including MassBank and MONA (Hilbig and Rarey, 2015) (see Supplemental Experimental Procedures).

2.11. Bioinformatics analysis

For the proteomics results, Gene ontology (GO) enrichment and Kyoto Encyclopedia of Genes and Genomes (KEGG) analysis were performed using DAVID online software. For the metabonomics results, multidimensional statistical analysis was performed using MetaboAnalyst software, including unsupervised principal component analysis (PCA), supervised partial least squares discriminant analysis (PLS-DA). Univariate statistical analysis was performed by Students' t-tests and KEGG pathway analysis was performed using MBROLE 2.0 online software.

3. Results

3.1. Identification and characteristics of CAP^r 1 and CAP^r 2 Mtb strains

To obtain CAP^r Mtb strains, wild type H37Rv Mtb strains were treated with CAP according to the route of Fig. 1. Sixty CAP^r Mtb strains (MIC > 2.5 μg/ml) were randomly selected for further characterization of CAP^r associated genes *tlyA* and *rrs* by sequencing. Among these CAP^r Mtb strains, 45 strains had the same point mutation in *tlyA* (695 G→A, G232D), and 12 strains had a frameshift *tlyA* mutation (357 G deletion) (Supplemental Table S1). In addition to the *tlyA* mutation, only three strains (3/60) were found to harbor *rrs* mutation (A1401 G). Moreover, we also constructed KAN^r and AMK^r Mtb strains induced by kanamycin and amikacin using the same method, respectively. In neither of KAN^r nor AMK^r Mtb strains, *tlyA* were mutated, while *rrs* (A1401 G) mutation were 100% (15/15) in AMK^r Mtb strains, and 87.5% (18/21) in KAN^r Mtb strains. Notably, all KAN^r and AMK^r Mtb strains with *rrs* (A1401 G) mutation were also resistant to CAP (data not shown), in consistence with reported laboratory and clinical results (Reeves et al., 2015; Sowajassatakul et al., 2014). These results suggested that *tlyA* mutation was the most direct domains in CAP^r Mtb strains.

Among the CAP^r Mtb strains, the *tlyA* deficient CAP^r Mtb strains (CAP^{r}1) occurs at a 20% frequency in nature and has a higher resistance to CAP (> 40 μg/ml) than does the *tlyA* point mutation CAP^r Mtb strains (CAP^{r}2) (G695A, 10 μg/ml). In addition, these two strains were not cross-resistant to 9 other anti-TB drugs except CAP (Supplemental Table S2). Furthermore, to verify whether the mutation was stable, we cultured both strains for three continuous generations without CAP and found the mutations and CAP resistance level unchanged (data not shown), indicating that the CAP^r strains have been successfully established.

Next, genome sequencing was performed on the CAP^{r}1, CAP^{r}2 and parental strains. Interestingly, comparative genomic analysis revealed that apart from the point mutation within *tlyA* of CAP^{r}2 strain, a missense mutation occurred in *plcC* (143 T→C, Q462R) compared to its parental strain. Different from CAP^{r}2, CAP^{r}1 had four different mutations: *tlyA* (357 G deletion), *Rv0228* (516C→G, A172 G), *PPE51* (259G→C, A87 P) and a synonymous mutation in *mtbA* (Supplemental Table S3). It is known that loss-of-function mutations in *tlyA* can confer CAP resistance in Mtb (Maus et al., 2005; Monshupanee et al., 2012) and the inactivating mutations in *tlyA* include two types: point and deficient. Although the locations of these mutations are different, the two kinds of mutations widely exist in laboratory CAP^r isolates (Engstrom et al., 2011; Hu et al., 2013; Maus et al., 2005). The CAP^r strains we induced fit the two types of mutations, but they were not found in reported clinical isolates. This discrepancy is likely related to fewer reported strains, different strain backgrounds, and their growth differences *in vivo* versus *in vitro*.

3.2. Global protein expression patterns of CAP^r 1 and CAP^r 2 Mtb strains

To further investigate the changes at protein levels of the strains caused by CAP, we performed global protein expression profiling on the CAP^{r}1, CAP^{r}2 strains and their parental strains. In total, 1,891 proteins were identified. For CAP^{r}1 strains, compared to its parent strain, a total of 166 differentially expressed 1.5-fold or greater change proteins were found (P < 0.05), including 61 down-regulated proteins and 105 up-regulated proteins, respectively (Supplementary Table S4). For the CAP^{r}2 strain, 22 proteins were identified, including 17 proteins that were upregulated and 5 proteins that were downregulated.

We further investigated the GO categories of the changed proteins using DAVID online software (Fig. 2). Among the increased proteins, in cellular component ontology, we found that the ribosome-associated proteins increased in both CAP^r strains, while the ribosomal protein species in the CAP^{r}1 strain increased significantly more than those of

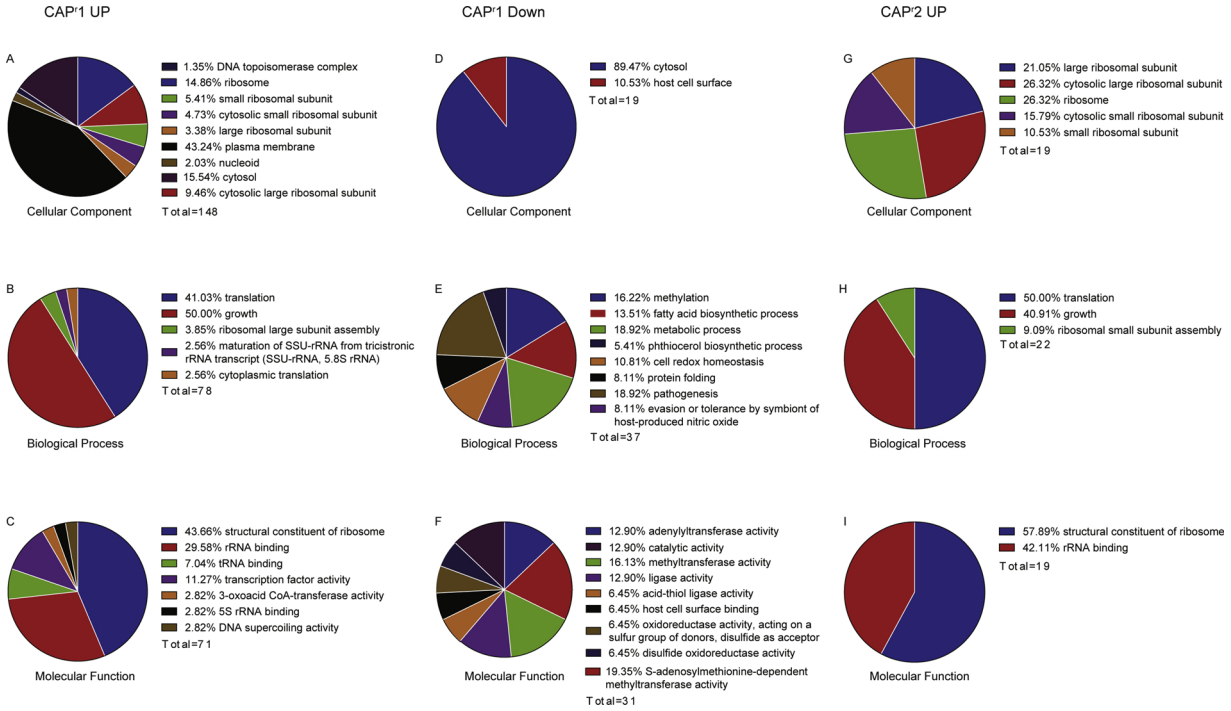

Fig. 2. Gene Ontology categories for the differentially expressed proteins of H37Rv in response to CAP using DAVID analysis. (A), (B) and (C) Functional classification of the CAP^r 1 upregulated proteins (1.5-fold change) in the biological processes, molecular functions, and cellular components, respectively. (D), (E) and (F) Functional classification of the CAP^r 1 downregulated proteins (1.5-fold change) in the biological processes, molecular functions, and cellular components, respectively. (G), (H) and (I) Functional classification of the CAP^r 2 upregulated proteins (1.5-fold change) in the biological processes, molecular functions, and cellular components, respectively.

the CAP^{r}2 strain (CAP^{r}1, 31 proteins; CAP^{r}2, 11 proteins) (Fig. 2A and G). Notably, there were also 64 proteins (43.24%) related to the plasma membrane in CAP^{r}1 strain (Fig. 2A). Accordingly, in the biological process ontology, the process of the translation, growth and ribosomal assembly were enriched in both CAP^r strains compared to their parent strain (Fig. 2B and H). The difference is that under the pressure of CAP, the changes of CAP^{r}1 focused on ribosomal large subunit assembly, while the changes of CAP^{r}2 tended to focus on small subunit assembly (Fig. 3A and B). The above results indicated that the CAP^r strain might grow faster than the parental strain. However, we observed that the two CAP^r strains had similar phenotype and growth characteristics (Fig. 4A and B) that a similar phenomenon has also been observed by other researchers (Johansen et al., 2006; Maus et al., 2005). Interestingly, in Congo red assay, we found that the cell surface of CAP^{r}1 strain is smoother than that of wild-type strain and CAP^{r}2 strain (Fig. 4A).

In the biological process ontology, the fatty acid biosynthetic process and metabolic process with decreased abundance were enriched in the CAP^r 1 strain (Fig. 2E), such as FadD9, FadD21, FadD26, FadD29, FadD34 and PpsE (Supplemental Table S4). In addition, PapA1, PapA3 and AcpM were also found decreased in CAP^r 1 strain. Sulfolipid-1 (SL-1) was the most abundant sulfatide in the family of cell surface sulfated lipids which were identified in Mtb extracts and correlated to bacterial virulence (Dubos and Middlebrook, 1948; Gangadharam et al., 1963; Middlebrook et al., 1959). *Kumar et al.* has proved that PapA1 is an essential acyltransferases for the biosynthesis of Sulfolipid-1(Kumar et al., 2007). Polyacyltrehalose (PAT), a pentaacylated trehalose-based glycolipid, is one of the components of Mtb cell wall. Hatzios SK et al. proved that PapA3 is involved in PAT assembly and leads to a decline in glycolipid biosynthesis (Hatzios et al., 2009). It has been previously shown that acpM is a major component of fatty acid synthase II in Mtb (Kremer et al., 2001).

Among the decreased proteins, we observed that ESAT-6, CFP-10 and other ESX family antigens (EsxN and EsxG) were significantly decreased in the CAP^r 1 strain (Supplemental Table S4). We also found the evasion or tolerance by symbiont of host-produced nitric oxide process and pathogenesis process were significantly reduced in the CAP^{r}1 strain, suggesting that the survival ability of the CAP^{r}1 strain in the host might be weakened (Fig. 2E). To verify this assumption, we tested the bacterial resistance to macrophages (murine RAW264.7 cell) and found that at 76 h post-infection, the CAP^{r}1 strain grew to a lower yield in macrophages than the control and CAP^r 2 strain (Fig. 4C). Md. Aejazur Rahman et al. had also reported that the *tlyA* protein negatively regulates T helper 1 (Th1) and Th17 differentiation and promotes TB pathogenesis. They also found that the *tlyA*-deficient Mtb exhibited reduced bacillary load in macrophages and mice compared to the wild-type strain (Rahman et al., 2015). Interestingly, we found the methylation process was dramatically repressed along with six reduced AdoMet-MTs (Rv0830, Rv0726c, Rv0415, Rv0416, Rv3767c and Rv1896c) (Fig. 2E). Notably, the decreased AdoMet-MTs were observed only in the *tlyA* deficient Mtb strain, not in the CAP^r 2 strain, suggesting that the CAP^r 1 strain has a more complex and effective drug-resistant mechanism than the CAP^r 2 strain.

3.3. Compared with tlyA point mutation CAP^{r}2 Mtb strains, lipid metabolism pathway was significantly enriched by downregulated intracellular metabolites in tlyA deficient CAP^{r}1 Mtb strains

As mentioned above, the relative abundance of some proteins involved in metabolism and fatty acid synthesis (ppsE, FadD21, FadD29, FadD26 and FadD34) in the CAP^{r}1 strain were significantly decreased while several proteins involved in glycerophospholipid metabolism and glycerolipid metabolism were observably increased (FbpB, PlcA, PlcB, FabG1 and Rv0223c) (Fig. 5). To investigate the metabolomics level in the CAP^{r}1 and CAP^{r}2 Mtb, the intracellular and extracellular metabolites were evaluated by liquid chromatography coupled with tandem mass spectrometry (LC–MS) and analyzed by multi- and univariate analyses. For multivariate analysis, PCA showed that 72.1% (CAP^{r}1) and 56.6% (CAP^{r}2) of the total variance in the data were represented by

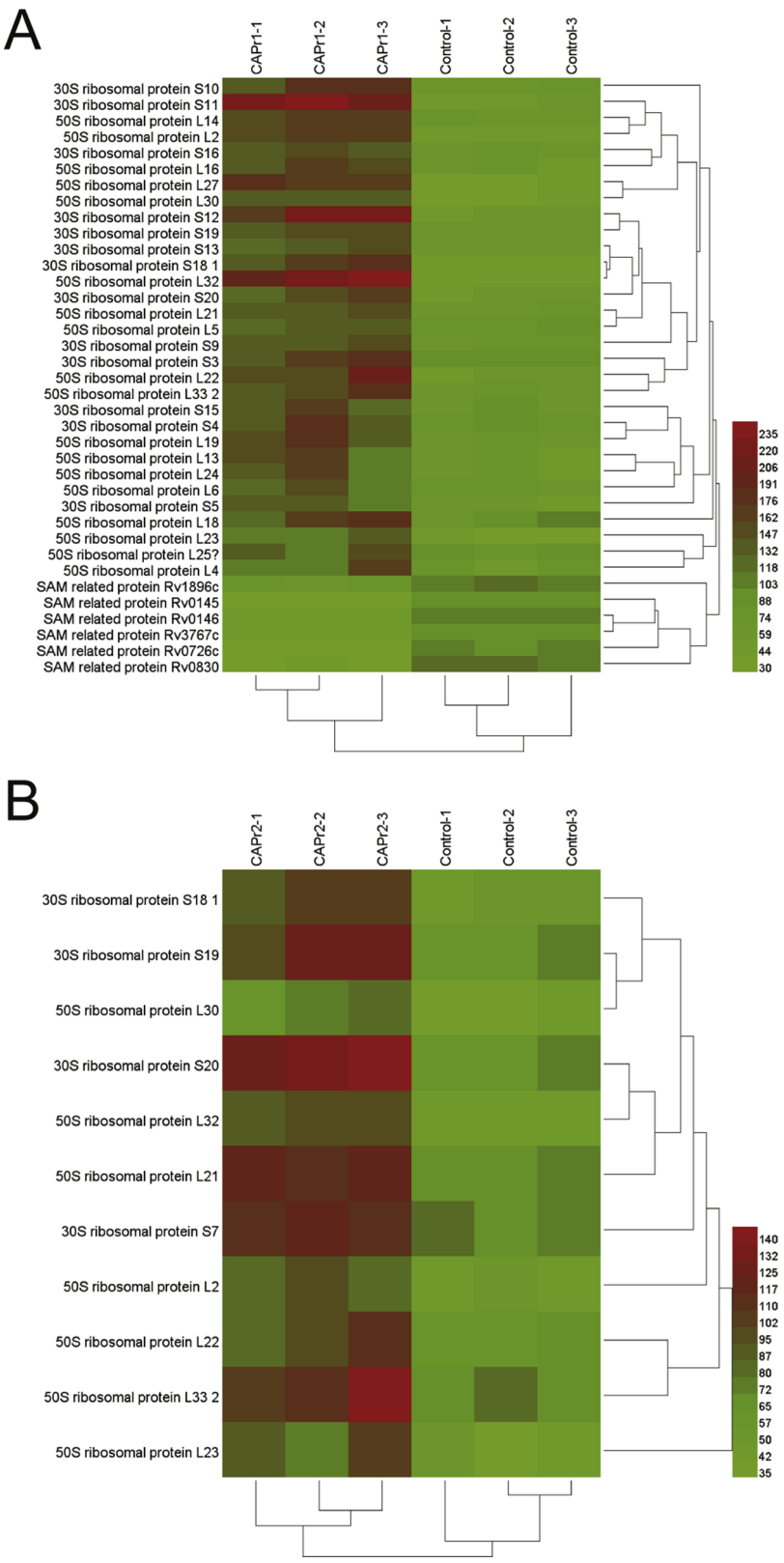

Fig. 3. Heat map showed the differentially expressed ribosomal proteins in CAP^r Mtb strains (1.5-fold changed).
(A)Heat map showing the average relative abundance of differentially expressed ribosomal proteins and S-adenosylmethionine-dependent methyltransferase related protein in CAP^r 1 Mtb. (B)Heat map comparing the abundances of differentially expressed ribosomal proteins in CAP^r 2 Mtb. Green and red indicate decreases and increases.

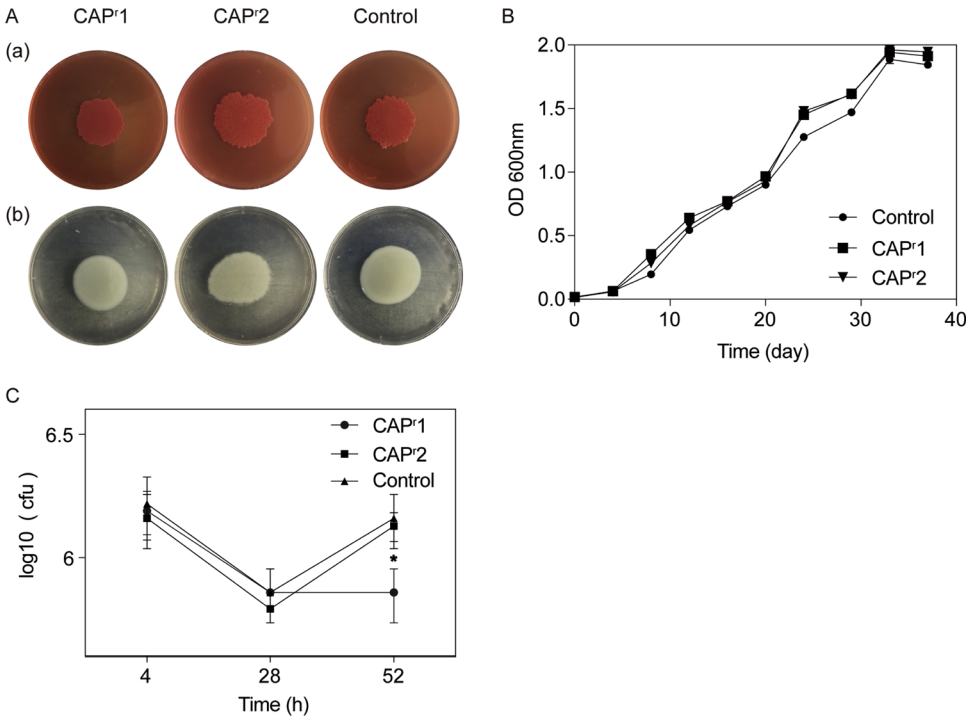

Fig. 4. Characterization of CAP-resistant Mtb used in this study. (A) Phenotypic analysis of *M. tuberculosis* strains. Wild-type strain (control) was compared to *tlyA* deficient CAP^r strains (CAP^{r}1) and *tlyA* site-mutated CAP^r strains (CAP^{r}2) for the following phenotypes: (a) Colony morphology, (b) Sliding motility. (B) Growth of *M. tuberculosis* H37Rv, CAP^r 1 and CAP^r 2 strains in 7H9 + ADC liquid media for 37 days. The average of two biological replicates is shown. (C) Bacterial load in the murine RAW264.7 cell. The macrophages were infected with CAP^r 1, CAP^r 2 and their parental strains, respectively. Error bars indicate standard errors for each group (n = 3).

the first three principal components compared to the control (Fig. 6A and B). The 3D-PCA score plot revealed that the CAP^r strains can be distinguished from the parental strain based on the first three principal components, with the CAP^r strains clearly separated from the parental strain along principal component 1, which represented 38.9% (CAP^{r}1) and 34.5% (CAP^{r}2) of the variance. In view of the significant separation achieved using PCA, supervised analysis PLS-DA (Fig. 6C and D) was subsequently performed to maximize the separation and to identify additional metabolites to those identified using PCA. In the PLS-DA score plot, the separation between different Mtb species is more

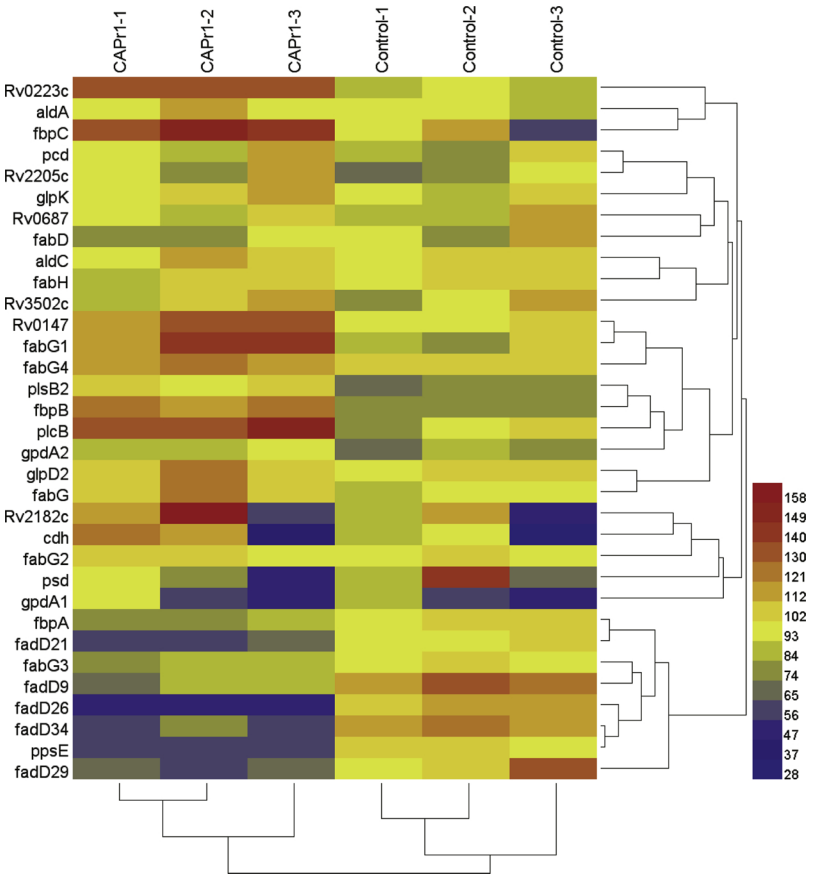

Fig. 5. Heat map showed the proteins involved in glycerophospholipid metabolism and glycerolipid metabolism in CAP^{r}1 Mtb strain. Purple and red indicate decreases and increases. Many identified proteins in CAP^{r}1 Mtb strain are associated with lipid metabolism. Among these proteins, some upregulated proteins are involved in the glycerophospholipid and glycerolipid metabolism, such as PlcA, PlcB, GlpD1, PlsB2, Rv2182c, Cdh, FbpB, FbpC. Besides, FadD26 and FadD29, which are involved in fatty acid synthesis, were down-regulated. (For interpretation of the references to colour in this figure legend, the reader is referred to the web version of this article).

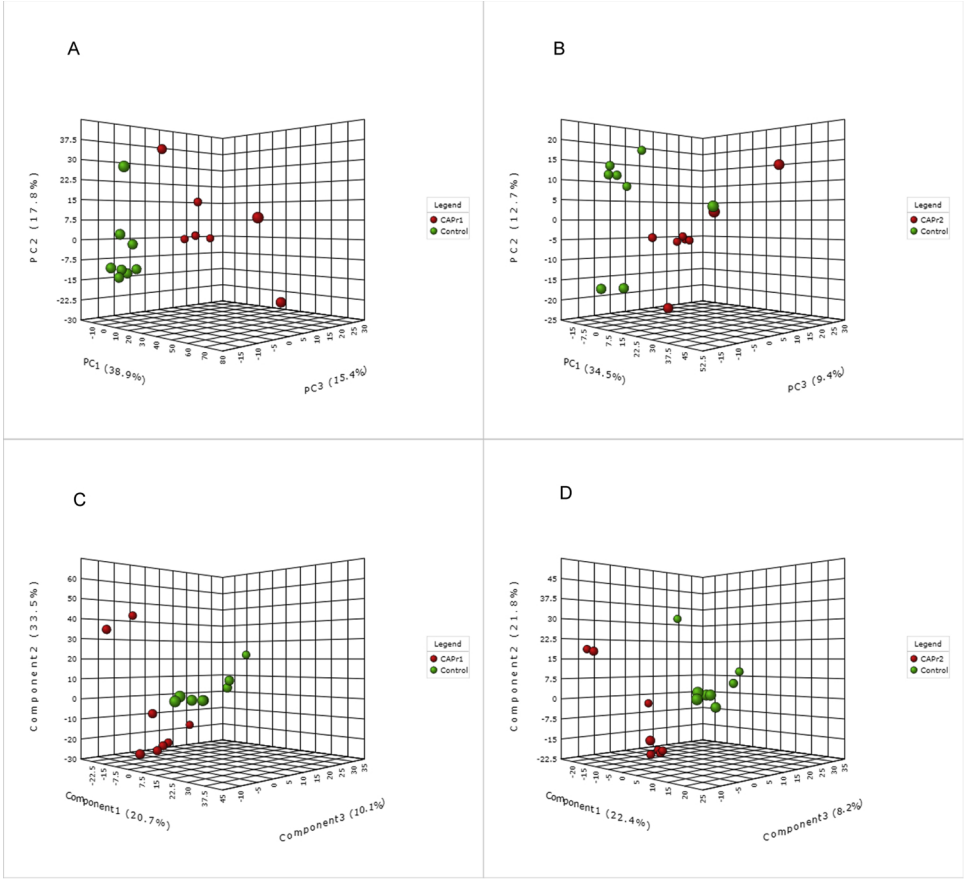

Fig. 6. PCA score plot and PLS-DA score plot based on intracellular metabolites of CAP^r strains compared with their parent strain. (A) PCA score plot of metabolite profiles of distinct developmental of CAP^{r}1. PCA presented as combination of first three dimensions, which together comprise 72.1% of the metabolite variance. (B) PCA Score plots of CAP^r 2. (C) PLS-DA score plot of metabolite profiles of distinct developmental of CAP^r 1. PLS-DA presented as combination of first three dimensions, which together comprise 64.3% of the metabolite variance. (D) PLS-DA plots of CAP^r 2. A web-based tool MetaboAnalyst 3.0 was used to analyze the data.

prominent. Potential metabolites were selected based on the VIP score (> 1). To further confirm the specificity and significance of potential metabolites identified from PCA and PLS-DA, univariate analysis of each metabolite was performed using Student's t-test. The potential metabolites contributing most to the variation between CAP^r and the parental strain with significantly higher level in PLS-DA was carried out for analysis. Of these differential compounds identified in the intracellular region of CAP^r 1 strain, 29 decreased metabolites were involved in membrane lipid formation and metabolism, viz. phosphatidic acid (PA), phosphatidylethanolamine (PE), phosphatidylcholine (PC), phosphatidylserine (PS), phosphatidylinositol (PI), phosphatidyl glycerin (PG) and diglyceride (DG), Monogalatosyl diglyceride (MGDG), digalactosyl diglyceride (DGDG), sulfoquinovosyl diacylglycerol (SQDG) (Supplemental Table S5). Next, we enriched the KEGG pathways of these altered metabolites by MBRole 2.0 online analysis. As shown in Supplemental Table S5, glycerolipid metabolism and glycerophospholipid metabolism pathway were the drastically altered metabolic activity in CAP^r 1 strain with considerable enrichment (FDR $<$ 0.01). In addition, we observed that cytidine-5'-triphosphate had an approximately 70-fold increase in the CAP^r 1 strain, and riboflavin was also upregulated by approximately 18-fold (Supplemental Table S5).

We also characterized the metabolomes of the culture supernatant of CAP^r strains by the same method used for testing the extracellular metabolites. Interestingly, we also detected a significant decrease in the relative abundance of lipids compared to the control (Supplemental Table S6). Notably, different from the CAP^{r}1 strain, no significant changes at individual metabolite levels in either cellular content or spent culture media of CAP^{r}2 strain were detected (data not shown), further indicating that the CAP^{r}1 strain has a CAP-resistant mechanism different from that of the CAP^{r}2 strain. We further enriched the KEGG pathways of these altered metabolites. Among the intracellular metabolites, there were only three significantly decreasing pathways, including glycerophospholipid metabolism, glycerolipid metabolism and metabolic pathways (Supplemental Table S5). As such, glycerophospholipid metabolism and the biosynthesis of unsaturated fatty acids were reduced in extracellular metabolites (Supplemental Table S6). Taken together, the above results illustrated that there was a substantial shift in lipid metabolism caused by CAP resulting in greater consumption of fatty acids.

4. Discussion

In this study, we screened and established two different CAP-resistant strains (*tlyA* deficient and point mutation) by increasing concentrations of CAP to Mtb *in vitro* and compared the differential proteins and metabolites of CAP-resistant Mtb and their parent strain using an integrated genomic-proteomic-metabonomic approach.

Different from the method induced by high concentration drugs (Zhao et al., 2014), a continuous drug concentration gradient induction (Fig. 1, Supplemental Experimental Procedures) can better simulate the accumulation of drugs in the body. Interestingly, among the reported CAP^r associated genes, we found there was an about 95% mutation rate in *tlyA* including 20% frameshift and 75% point-mutation, as well as 5% point mutation (A1401 G) in *rrs* gene (Supplemental Table S1). We also found that in KAN^r and AMK^r Mtb strains constructed using the same method, there were high mutation rates in *rrs* gene while *tlyA* were not mutated in these strains. Since *rrs* A1401 G allele are reported as a marker of cross-resistance to CAP, amikacin and kanamycin, our results showed that all KAN^r and AMK^r Mtb strains with *rrs* (A1401 G) mutation were indeed resistant to CAP. Therefore, we speculate that *tlyA* gene is the direct target of CAP, and *rrs* gene may be the direct target of kanamycin and amikacin. As for why *rrs* mutation can also cause CAP resistance in Mtb, it remains to be studied. Given that amikacin and kanamycin are recommended as the first choice among the second-line

injectable anti-TB drugs and these two drugs can cause high frequency mutation of *rrs* (A1401 G) inducing cross-resistance at the same time, which can explain why the mutation rate of *rrs* is much higher than that of *tlyA* in CAP drug-resistant strains clinically.

We further investigated the proteomic changes between the two CAP-resistant strains. Interestingly, our results showed that there were a lot of ribosomal proteins increased in these strains. Some previous studies also reported that the ribosomal subunits have been dramatically enriched in the drug-resistant group (Belenky et al., 2015; Lin et al., 2014a). For example, oxytetracycline which has a broad spectrum of anti-pathogenic microorganisms and belongs to the class of tetracyclines (Lin et al., 2015), the researchers have found that some translation related ribosomal subunits, such as S17, L27, S18, S19, S16, and S20, were obviously increased in oxytetracycline-resistant bacteria. In addition, some aminoglycoside drug-resistant hospital isolates *Enterococcus faecium* and *Neisseria gonorrhoeae* also have a lot of ribosomal subunits significantly increased, compared to drug-sensitive strains (Nabu et al., 2014; Wagner et al., 2018). Therefore, it can be validated that any antibiotic that acts on microbial ribosomes will increase ribosome protein expression when bacteria are resistant. We also analyzed the KEGG pathways of differentially expressed proteins in Mtb (Supplementary Table S4). Only the ribosomal pathway was enriched with increased proteins in both CAP^r strains, suggesting the important role of ribosome in overcoming the pressure caused by CAP since this drug inhibits protein synthesis. A microarray-based study on CAP also showed that the treatment of Mtb with CAP resulted in overexpression of several ribosomal proteins (Fu and Shinnick, 2007). Yuan Lin et al. had further reported that the overproduction of ribosomal protein L12 in Mtb, but not L10, could lower the antibacterial activity of T766 and T054, which are two anti-TB drugs, indicating that the ribosome was likely the cellular target (Lin et al., 2012). They also found an overexpression of L12 and/or L10 in *M. smegmatis*, which enabled the increase of the CAP MIC (Lin et al., 2014b). Our results confirm the conclusion that the promotion of ribosomal subunits may be a compensative tactic for bacterial defense to antibiotics, and further indicate that more ribosomal subunits responsible for antibiotic resistance may be revealed by high-throughput proteomics.

In addition, several AdoMet-MTs (Rv0830, Rv0726c, Rv0415, Rv0416, Rv3767c and Rv1896c) were significantly decreased in *tlyA* deficient Mtb strains. It is known that CAP resistance in Mtb increases through the inactivation of AdoMet-MT activity of *tlyA*, which can direct 2′-*O*-methylation on ribosomal subunits (Monshupanee et al., 2012). Our results indicated that the increased CAP resistance may not only depend on *tlyA* but also be due to the reducing action of AdoMet-MTs, which could not compensate for the effect caused by *tlyA* deletion.

Another interest finding in *tlyA* deficient CAP^{r}1 Mtb is that the glycerophospholipid metabolism and glycerolipid metabolism pathway were enriched at the level of both proteome and metabolome (Supplemental Tables S4, S5 and S6). Recent studies have shown that bacterial membrane anionic lipids are promising targets to fight antimicrobial resistance, such as in aminoglycoside antibiotics. A transcriptomic study on the mechanism of action of CAP additionally revealed substantial changes in a variety of other gene classes, including lipid metabolism, cell wall and cell processes, and intermediary metabolism and respiration in Mtb (Fu and Shinnick, 2007). Another study revealed more dramatic changes in the mycomembrane of *M. smegmatis* in response to challenge with CAP (Man et al., 2018). They propose that CAP could act by inhibiting protein synthesis but induce substantial remodeling of the mycomembrane. In addition, they presented a substantial shift in metabolism following CAP challenge, resulting in a greater consumption of fatty acids, a depletion of mycolic acid and a rigidification of the mycomembrane as trehalose monomycolate predominates over trehalose dimycolate. This hypothesis is partially supported by our results regarding the proteomics and LC–MS metabolomics of the CAP^{r}1 strain.

Compared to wild type strain, many proteins with significant differential expression in CAP^{r}1 strain involved in fatty acid synthesis, glycerophospholipid metabolism and glycerolipid metabolism (Fig. 5, Supplemental Tables S4, S5 and S6), such as FadD proteins and Plc proteins. In Mtb, 34 *fadD* genes are annotated as members of the adenylate-forming superfamily (Camus et al., 2002) and several *fadD* genes involved in the synthesis of bioactive lipids have been shown to be essential for bacterial survival or virulence (Dunphy et al., 2010; Liu et al., 2013; Rindi et al., 2004; Simeone et al., 2010). Phthiocerol dimycocerosate (PDIM) is one of the cell wall lipids of mycobacteria. The genes *tesA*, *fadD26*, *ppsABCDE*, *mas*, *fadD28* could involve in the synthesis of PDIM (Chavadi et al., 2011, 2012; Vergnolle et al., 2015). Phthiocerol dimycocerosates (DIMs) and phenolic glycolipids (PGLs) are two structurally related families of the surface-exposed lipids, which have been proved contribute to the cell envelope permeability barrier and virulence (Astarie-Dequeker et al., 2009; Cox et al., 1999). Roxane Siméone et al. have clearly demonstrated that FadD29 is an essential active intermediates during the formation of PGLs, and FadD26 is required for the production of DIMs (Simeone et al., 2010).

Many up-regulated proteins in CAP^r 1 strain, such as FbpB, PlcA, PlcB, FabG1 and Rv0223c, are involved in cell wall synthesis and lipid metabolism. The antigen 85(Ag85)proteins (encoded by the genes *fbpA*, *fbpB*, and *fbpC*) have been found to possess mycolyltransferase activity and may play a role in cell wall synthesis (Azad et al., 1997, 1996; Banerjee et al., 1994; Blanchard, 1996). Belisle et al. have proved Ag85 is responsible for the transfer of mycolic acids to α-α′-trehalose to form α-α′-trehalose monomycolate (TMM) and α-α′-trehalose dimycolate (TDM) (Belisle et al., 1997). Mycolic acids are very long-chain α-branched β-hydroxylated fatty acids (C54–63), which protect Mtb from other hazards (Takayama et al., 2005). Mycolic acid biosynthesis includes a combination of type II fatty acid synthase (FAS-II) (Bloch, 1977). Hedia et al. proved that FabG1 belongs to the mycobacterial FAS-II system (Marrakchi et al., 2002). Phospholipase C1 (plcA) and phospholipase C2 (plcB) are involved in the metabolism of glycerophospholipid metabolism in Mtb (Johansen et al., 1996; Raynaud et al., 2002). In addition, Rv0223c could play a role in the glycerolipid metabolism (Kim et al., 2009).

Many lipids in intracellular and extracellular metabolites are indeed significantly reduced (Fig. 7). We did not find mycolic acid and trehalose monomycolate, which may be ascribed to different methods for detecting metabolites. Thus, it can be seen that the glycerophospholipid metabolism and glycerolipid metabolism are related to the drug resistance of pathogenic bacteria, but how does it affect the drug resistance of Mtb need further study.

In this study, we generated two different CAP^r strains (*tlyA* deficient CAP^{r}1 Mtb strains and *tlyA* point mutation CAP^{r}2 Mtb strains) *in vitro* using increasing concentrations of CAP, and used an integrated genomic-proteomic-metabonomic approach to compare differences in genomic, proteins and metabolites of different CAP^r Mtb strains and their parent strain. We found that CAP^{r}1 and CAP^{r}2 Mtb strains have different CAP resistance mechanisms. Aside from the inactivation of *tlyA*, *tlyA* deficient CAP^{r}1 Mtb strains exhibited greater drug tolerance than CAP^{r}2 strains may be associated with the weakening of AdoMet-MTs activity and abnormal membrane lipid metabolism such as inhibiting fatty acid metabolism but promoting glycolipid phospholipid and glycerolipid metabolism. These studies reveal a new mechanism for CAP resistance to tlyA deficient or mutation Mtb strains, and may be helpful in developing new therapeutic approaches to prevent Mtb resistance to CAP.

Funding statement

This work was supported by the National Infectious Disease Science and Technology Major Projects (2018zx10103001, 201710201302), the National Natural Science Foundation of China (Grant No. 31800129), and the Science and Technology Planning Project of Guangzhou (201604020006).

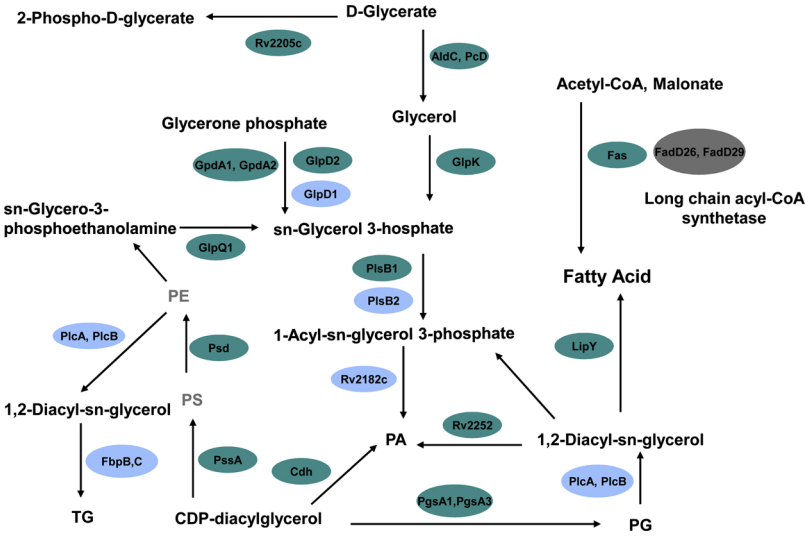

Fig. 7. A schematic summary of lipid metabolism obtained in this study. A schematic summary of the metabolic and proteomic changes involved in glycerolipid metabolism and glycerophospholipid metabolism in CAP^{r}1 Mtb strains. The black characters represent the different metabolites found in the CAP^{r}1 Mtb strain and gray characters indicate significantly decreased metabolites. The ellipse represents the different protein found in the CAP^{r}1 Mtb strain. Gray ellipse indicates significantly decreased protein and blue ellipse indicates increased protein (P value < 0.05 and 1.2-fold changes). PE, Phosphatidylethanolamine; PS, Phosphatidylserine; PG, Phosphatidylglycerol; TG, Triacylglycerol. (For interpretation of the references to colour in this figure legend, the reader is referred to the web version of this article).

Author contributions statement

W.J.W and T.C conceived, designed and supervised the overall study. L.Z and T.C acquired funding and supervised and administered the project. Z.Y.L provided the mutated mycobacterial strains. J.Z and H.M.Y collected and verified the mycobacterial strains. Y.M.C and C.C.Z coordinated the experiments to proceed smoothly. J.Z and H.M.Y processed the samples and performed the experiments. W.J.W, J.Z and Y.Z analyzed the data. W.J.W, J.Z, J.C.Z and Y.Z wrote the paper. All authors read and approved the final manuscript.

Data availability

The datasets generated during and/or analyzed during the current study are available from the corresponding authors upon request.

Acknowledgements

The authors express appreciation of Haicheng Li from Center for Tuberculosis Control of Guangdong Province for his advice and help in inducing CAP-resistant Mtb strains, to Jinfei Lin and Rurui Cen from Longsee (Guangzhou) Biomed Co. Ltd. for help with metabolomics analysis.

Appendix A. Supplementary data

Supplementary material related to this article can be found, in the online version, at doi:https://doi.org/10.1016/j.ijmm.2019.06.003.

References

Akbergenov, R., Shcherbakov, D., Matt, T., Duscha, S., Meyer, M., Wilson, D.N., Bottger, E.C., 2011. Molecular basis for the selectivity of antituberculosis compounds capreomycin and viomycin. Antimicrob. Agents Chemother. 55, 4712–4717.
Astarie-Dequeker, C., Le Guyader, L., Malaga, W., Seaphanh, F.K., Chalut, C., Lopez, A., Guilhot, C., 2009. Phthiocerol dimycocerosates of M. Tuberculosis participate in macrophage invasion by inducing changes in the organization of plasma membrane lipids. PLoS Pathog. 5, e1000289.
Azad, A.K., Sirakova, T.D., Fernandes, N.D., Kolattukudy, P.E., 1997. Gene knockout reveals a novel gene cluster for the synthesis of a class of cell wall lipids unique to pathogenic mycobacteria. J. Biol. Chem. 272, 16741–16745.
Azad, A.K., Sirakova, T.D., Rogers, L.M., Kolattukudy, P.E., 1996. Targeted replacement of the mycocerosic acid synthase gene in Mycobacterium bovis BCG produces a mutant that lacks mycosides. Proc. Natl. Acad. Sci. U. S. A. 93, 4787–4792.
Banerjee, A., Dubnau, E., Quemard, A., Balasubramanian, V., Um, K.S., Wilson, T., Collins, D., de Lisle, G., Jacobs Jr., W.R., 1994. inhA, a gene encoding a target for isoniazid and ethionamide in Mycobacterium tuberculosis. Science 263, 227–230.
Belenky, P., Ye, J.D., Porter, C.B., Cohen, N.R., Lobritz, M.A., Ferrante, T., Jain, S., Korry, B.J., Schwarz, E.G., Walker, G.C., Collins, J.J., 2015. Bactericidal antibiotics induce toxic metabolic perturbations that lead to cellular damage. Cell Rep. 13, 968–980.
Belisle, J.T., Vissa, V.D., Sievert, T., Takayama, K., Brennan, P.J., Besra, G.S., 1997. Role of the major antigen of Mycobacterium tuberculosis in cell wall biogenesis. Science 276, 1420–1422.
Blanchard, J.S., 1996. Molecular mechanisms of drug resistance in Mycobacterium tuberculosis. Annu. Rev. Biochem. 65, 215–239.
Bloch, K., 1977. Control mechanisms for fatty acid synthesis in Mycobacterium smegmatis. Adv. Enzymol. Relat. Areas Mol. Biol. 45, 1–84.
Caminero, J.A., Sotgiu, G., Zumla, A., Migliori, G.B., 2010. Best drug treatment for multidrug-resistant and extensively drug-resistant tuberculosis. Lancet Infect. Dis. 10, 621–629.
Camus, J.C., Pryor, M.J., Medigue, C., Cole, S.T., 2002. Re-annotation of the genome sequence of Mycobacterium tuberculosis H37Rv. Microbiology 148, 2967–2973.
Chavadi, S.S., Edupuganti, U.R., Vergnolle, O., Fatima, I., Singh, S.M., Soll, C.E., Quadri, L.E., 2011. Inactivation of tesA reduces cell wall lipid production and increases drug susceptibility in mycobacteria. J. Biol. Chem. 286, 24616–24625.
Chavadi, S.S., Onwueme, K.C., Edupuganti, U.R., Jerome, J., Chatterjee, D., Soll, C.E., Quadri, L.E., 2012. The mycobacterial acyltransferase PapA5 is required for biosynthesis of cell wall-associated phenolic glycolipids. Microbiology 158, 1379–1387.
Cox, J.S., Chen, B., McNeil, M., Jacobs Jr., W.R., 1999. Complex lipid determines tissue-specific replication of Mycobacterium tuberculosis in mice. Nature 402, 79–83.
Deshayes, C., Laval, F., Montrozier, H., Daffe, M., Etienne, G., Reyrat, J.M., 2005. A glycosyltransferase involved in biosynthesis of triglycosylated glycopeptidolipids in Mycobacterium smegmatis: impact on surface properties. J. Bacteriol. 187, 7283–7291.
Dubos, R.J., Middlebrook, G., 1948. Cytochemical reaction of virulent tubercle bacilli. Am. Rev. Tuberc. 58, 698.
Dunphy, K.Y., Senaratne, R.H., Masuzawa, M., Kendall, L.V., Riley, L.W., 2010. Attenuation of Mycobacterium tuberculosis functionally disrupted in a fatty acyl-coenzyme A synthetase gene fadD5. J. Infect. Dis. 201, 1232–1239.
Engstrom, A., Perskvist, N., Werngren, J., Hoffner, S.E., Jureen, P., 2011. Comparison of clinical isolates and in vitro selected mutants reveals that tlyA is not a sensitive genetic marker for capreomycin resistance in Mycobacterium tuberculosis. J. Antimicrob. Chemother. 66, 1247–1254.
Falzon, D., Jaramillo, E., Schunemann, H.J., Arentz, M., Bauer, M., Bayona, J., Blanc, L., Caminero, J.A., Daley, C.L., Duncombe, C., Fitzpatrick, C., Gebhard, A., Getahun, H., Henkens, M., Holtz, T.H., Keravec, J., Keshavjee, S., Khan, A.J., Kulier, R., Leimane, V., Lienhardt, C., Lu, C., Mariandyshev, A., Migliori, G.B., Mirzayev, F., Mitnick, C.D., Nunn, P., Nwagboniwe, G., Oxlade, O., Palmero, D., Pavlinac, P., Quelapio, M.I., Raviglione, M.C., Rich, M.L., Royce, S., Rusch-Gerdes, S., Salakaia, A., Sarin, R., Sculier, D., Varaine, F., Vitoria, M., Walson, J.L., Wares, F., Weyer, K., White, R.A., Zignol, M., 2011. WHO guidelines for the programmatic management of drug-resistant tuberculosis: 2011 update. Eur. Respir. J. 38, 516–528.
Fu, L.M., Shinnick, T.M., 2007. Genome-wide exploration of the drug action of capreomycin on Mycobacterium tuberculosis using Affymetrix oligonucleotide GeneChips. J. Infect. 54, 277–284.
Gangadharam, P.R., Cohn, M.L., Middlebrook, G., 1963. Infectivity, Pathogenicity and Sulpholipid Fraction of Some Indian and British Strains of Tubercle Bacilli. Tubercle 44, 452–455.
Hatzios, S.K., Schelle, M.W., Holsclaw, C.M., Behrens, C.R., Botyanszki, Z., Lin, F.L., Carlson, B.L., Kumar, P., Leary, J.A., Bertozzi, C.R., 2009. PapA3 is an acyltransferase required for polyacyltrehalose biosynthesis in Mycobacterium tuberculosis. J. Biol. Chem. 284, 12745–12751.
Hilbig, M., Rarey, M., 2015. MONA 2: a light cheminformatics platform for interactive compound library processing. J. Chem. Inf. Model. 55, 2071–2078.
Hu, Y., Hoffner, S., Wu, L., Zhao, Q., Jiang, W., Xu, B., 2013. Prevalence and genetic characterization of second-line drug-resistant and extensively drug-resistant Mycobacterium tuberculosis in Rural China. Antimicrob. Agents Chemother. 57, 3857–3863.

Johansen, K.A., Gill, R.E., Vasil, M.L., 1996. Biochemical and molecular analysis of phospholipase C and phospholipase D activity in mycobacteria. Infect. Immun. 64, 3259–3266.
Johansen, S.K., Maus, C.E., Plikaytis, B.B., Douthwaite, S., 2006. Capreomycin binds across the ribosomal subunit interface using tlyA-encoded 2'-O-methylations in 16S and 23S rRNAs. Mol. Cell 23, 173–182.
Kim, C.Y., Webster, C., Roberts, J.K., Moon, J.H., Alipio Lyon, E.Z., Kim, H., Yu, M., Hung, L.W., Terwilliger, T.C., 2009. Analysis of nucleoside-binding proteins by ligand-specific elution from dye resin: application to Mycobacterium tuberculosis aldehyde dehydrogenases. J. Struct. Funct. Genomics 10, 291–301.
Kim, S.J., Hong, Y.P., 1992. Drug resistance of Mycobacterium tuberculosis in Korea. Tuber. Lung Dis. 73, 219–224.
Kremer, L., Nampoothiri, K.M., Lesjean, S., Dover, L.G., Graham, S., Betts, J., Brennan, P.J., Minnikin, D.E., Locht, C., Besra, G.S., 2001. Biochemical characterization of acyl carrier protein (AcpM) and malonyl-CoA:AcpM transacylase (mtFabD), two major components of Mycobacterium tuberculosis fatty acid synthase II. J. Biol. Chem. 276, 27967–27974.
Kumar, P., Schelle, M.W., Jain, M., Lin, F.L., Petzold, C.J., Leavell, M.D., Leary, J.A., Cox, J.S., Bertozzi, C.R., 2007. PapA1 and PapA2 are acyltransferases essential for the biosynthesis of the Mycobacterium tuberculosis virulence factor sulfolipid-1. Proc. Natl. Acad. Sci. U. S. A. 104, 11221–11226.
Larsen, M.H., Biermann, K., Tandberg, S., Hsu, T., Jacobs Jr., W.R., 2007. Genetic manipulation of Mycobacterium tuberculosis. Curr. Protoc. Microbiol. 12 Chapter 10, Unit 10A.
Lau, S.K., Lam, C.W., Curreem, S.O., Lee, K.C., Lau, C.C., Chow, W.N., Ngan, A.H., To, K.K., Chan, J.F., Hung, I.F., Yam, W.C., Yuen, K.Y., Woo, P.C., 2015. Identification of specific metabolites in culture supernatant of Mycobacterium tuberculosis using metabolomics: exploration of potential biomarkers. Emerg. Microbes Infect. 4, e6.
Lin, X., Lin, L., Yao, Z., Li, W., Sun, L., Zhang, D., Luo, J., Lin, W., 2015. An integrated quantitative and targeted proteomics reveals fitness mechanisms of Aeromonas hydrophila under oxytetracycline stress. J. Proteome Res. 14, 1515–1525.
Lin, X.M., Kang, L.Q., Li, H., Peng, X.X., 2014a. Fluctuation of multiple metabolic pathways is required for Escherichia coli in response to chlortetracycline stress. Mol. Biosyst. 10, 901–908.
Lin, Y., Li, Y., Zhu, N., Han, Y., Jiang, W., Wang, Y., Si, S., Jiang, J., 2014b. The anti-tuberculosis antibiotic capreomycin inhibits protein synthesis by disrupting interaction between ribosomal proteins L12 and L10. Antimicrob. Agents Chemother. 58, 2038–2044.
Lin, Y., Li, Y., Zhu, Y., Zhang, J., Li, Y., Liu, X., Jiang, W., Yu, S., You, X.F., Xiao, C., Hong, B., Wang, Y., Jiang, J.D., Si, S., 2012. Identification of antituberculosis agents that target ribosomal protein interactions using a yeast two-hybrid system. Proc. Natl. Acad. Sci. U. S. A. 109, 17412–17417.
Liu, Z., Ioerger, T.R., Wang, F., Sacchettini, J.C., 2013. Structures of Mycobacterium tuberculosis FadD10 protein reveal a new type of adenylate-forming enzyme. J. Biol. Chem. 288, 18473–18483.
Loots du, T., 2016. New insights into the survival mechanisms of rifampicin-resistant Mycobacterium tuberculosis. J. Antimicrob. Chemother. 71, 655–660.
Luies, L., du Preez, I., Loots, D.T., 2017a. The role of metabolomics in tuberculosis treatment research. Biomark. Med. 11, 1017–1029.
Luies, L., Reenen, M.V., Ronacher, K., Walzl, G., Loots, D.T., 2017b. Predicting tuberculosis treatment outcome using metabolomics. Biomark. Med.
Man, D.K., Kanno, T., Manzo, G., Robertson, B.D., Lam, J.K.W., Mason, A.J., 2018. Rifampin- or capreomycin-induced remodeling of the Mycobacterium smegmatis mycolic acid layer is mitigated in synergistic combinations with cationic antimicrobial peptides. mSphere 3.
Marrakchi, H., Ducasse, S., Labesse, G., Montrozier, H., Margeat, E., Emorine, L., Charpentier, X., Daffe, M., Quemard, A., 2002. MabA (FabG1), a Mycobacterium tuberculosis protein involved in the long-chain fatty acid elongation system FAS-II. Microbiology 148, 951–960.
Maus, C.E., Plikaytis, B.B., Shinnick, T.M., 2005. Mutation of tlyA confers capreomycin resistance in Mycobacterium tuberculosis. Antimicrob. Agents Chemother. 49, 571–577.
Mengatto, L., Chiani, Y., Imaz, M.S., 2006. Evaluation of rapid alternative methods for drug susceptibility testing in clinical isolates of Mycobacterium tuberculosis. Mem. Inst. Oswaldo Cruz 101, 535–542.
Middlebrook, G., Coleman, C.M., Schaefer, W.B., 1959. Sulfolipid from virulent tubercle Bacilli. Proc. Natl. Acad. Sci. U. S. A. 45, 1801–1804.
Monshupanee, T., Johansen, S.K., Dahlberg, A.E., Douthwaite, S., 2012. Capreomycin susceptibility is increased by TlyA-directed 2'-O-methylation on both ribosomal subunits. Mol. Microbiol. 85, 1194–1203.
Nabu, S., Lawung, R., Isarankura-Na-Ayudhya, P., Isarankura-Na-Ayudhya, C., Roytrakul, S., Prachayasittikul, V., 2014. Reference map and comparative proteomic analysis of Neisseria gonorrhoeae displaying high resistance against spectinomycin. J. Med. Microbiol. 63, 371–385.
Rahman, M.A., Sobia, P., Dwivedi, V.P., Bhawsar, A., Singh, D.K., Sharma, P., Moodley, P., Van Kaer, L., Bishai, W.R., Das, G., 2015. Mycobacterium tuberculosis TlyA protein negatively regulates t helper (Th) 1 and Th17 differentiation and promotes tuberculosis pathogenesis. J. Biol. Chem. 290, 14407–14417.
Raynaud, C., Guilhot, C., Rauzier, J., Bordat, Y., Pelicic, V., Manganelli, R., Smith, I., Gicquel, B., Jackson, M., 2002. Phospholipases C are involved in the virulence of Mycobacterium tuberculosis. Mol. Microbiol. 45, 203–217.
Reeves, A.Z., Campbell, P.J., Willby, M.J., Posey, J.E., 2015. Disparities in capreomycin resistance levels associated with the rrs A1401G mutation in clinical isolates of Mycobacterium tuberculosis. Antimicrob. Agents Chemother. 59, 444–449.
Rindi, L., Bonanni, D., Lari, N., Garzelli, C., 2004. Requirement of gene fadD33 for the growth of Mycobacterium tuberculosis in a hepatocyte cell line. New Microbiol. 27, 125–131.
Simeone, R., Leger, M., Constant, P., Malaga, W., Marrakchi, H., Daffe, M., Guilhot, C., Chalut, C., 2010. Delineation of the roles of FadD22, FadD26 and FadD29 in the biosynthesis of phthiocerol dimycocerosates and related compounds in Mycobacterium tuberculosis. FEBS J. 277, 2715–2725.
Sonden, B., Kocincova, D., Deshayes, C., Euphrasie, D., Rhayat, L., Laval, F., Frehel, C., Daffe, M., Etienne, G., Reyrat, J.M., 2005. Gap, a mycobacterial specific integral membrane protein, is required for glycolipid transport to the cell surface. Mol. Microbiol. 58, 426–440.
Sowajassatakul, A., Prammananan, T., Chaiprasert, A., Phunpruch, S., 2014. Molecular characterization of amikacin, kanamycin and capreomycin resistance in M/XDR-TB strains isolated in Thailand. BMC Microbiol. 14, 165.
Stanley, R.E., Blaha, G., Grodzicki, R.L., Strickler, M.D., Steitz, T.A., 2010. The structures of the anti-tuberculosis antibiotics viomycin and capreomycin bound to the 70S ribosome. Nat. Struct. Mol. Biol. 17, 289–293.
Takayama, K., Wang, C., Besra, G.S., 2005. Pathway to synthesis and processing of mycolic acids in Mycobacterium tuberculosis. Clin. Microbiol. Rev. 18, 81–101.
Vergnolle, O., Chavadi, S.S., Edupuganti, U.R., Mohandas, P., Chan, C., Zeng, J., Kopylov, M., Angelo, N.G., Warren, J.D., Soll, C.E., Quadri, L.E., 2015. Biosynthesis of cell envelope-associated phenolic glycolipids in Mycobacterium marinum. J. Bacteriol. 197, 1040–1050.
Vranakis, I., Goniotakis, I., Psaroulaki, A., Sandalakis, V., Tselentis, Y., Gevaert, K., Tsiotis, G., 2014. Proteome studies of bacterial antibiotic resistance mechanisms. J. Proteomics 97, 88–99.
Wagner, T., Joshi, B., Janice, J., Askarian, F., Skalko-Basnet, N., Hagestad, O.C., Mekhlif, A., Wai, S.N., Hegstad, K., Johannessen, M., 2018. Enterococcus faecium produces membrane vesicles containing virulence factors and antimicrobial resistance related proteins. J. Proteomics 187, 28–38.
Wang, X.D., Gu, J., Wang, T., Bi, L.J., Zhang, Z.P., Cui, Z.Q., Wei, H.P., Deng, J.Y., Zhang, X.E., 2011. Comparative analysis of mycobacterial NADH pyrophosphatase isoforms reveals a novel mechanism for isoniazid and ethionamide inactivation. Mol. Microbiol. 82, 1375–1391.
WHO, 2017. Global Tuberculosis Report 2017.
Zhao, F., Wang, X.D., Erber, L.N., Luo, M., Guo, A.Z., Yang, S.S., Gu, J., Turman, B.J., Gao, Y.R., Li, D.F., Cui, Z.Q., Zhang, Z.P., Bi, L.J., Baughn, A.D., Zhang, X.E., Deng, J.Y., 2014. Binding pocket alterations in dihydrofolate synthase confer resistance to para-aminosalicylic acid in clinical isolates of Mycobacterium tuberculosis. Antimicrob. Agents Chemother. 58, 1479–1487.